Light absorption of brown carbon aerosol in the PRD region of China

J.-F. Yuan, X.-F. Huang, L.-M. Cao, J. Cui, Q. Zhu, C.-N. Huang, Z.-J. Lan, and L.-Y. He

Key Laboratory for Urban Habitat Environmental Science and Technology, School of Environment and Energy, Peking University Shenzhen Graduate School, Shenzhen 518055, China

Corresponding author. Tel.: +86 755 26032532; Fax: +86 755 26035332.

E-mail address: huangxf@pku.edu.cn (X.-F. Huang).

Abstract: The strong spectral dependence of light absorption of brown carbon (BrC) aerosol is regarded to influence aerosol's radiative forcing significantly. The Absorption Angstrom Exponent (AAE) method has been widely used in previous studies to attribute light absorption of BrC at shorter wavelengths for ambient aerosols, with a theoretical assumption that the AAE of "pure" black carbon (BC) aerosol equals to 1.0. In this study, the AAE method was applied to both urban and rural environments in the Pearl River Delta (PRD) region of China, with an improvement of constraining the realistic AAE of "pure" BC through statistical analysis of on-line measurement data. A three-wavelength photo-acoustic soot spectrometer (PASS-3) and aerosol mass spectrometers (AMS) were used to explore the relationship between the measured AAE and the relative abundance of organic aerosol to BC. The regression and extrapolation analysis revealed that more realistic AAE values for "pure" BC aerosol ($AAE_{\_BC}$) were 0.86, 0.82, and 1.02 between 405 and 781 nm, and 0.70, 0.71, and 0.86 between 532 and 781 nm, in the campaigns of $urban_{\_winter}$, $urban_{\_fall}$, and $rural_{\_fall}$, respectively. Roadway tunnel experiments were conducted and the results further confirmed the representativeness of the obtained $AAE_{\_BC}$ values for the urban environment. Finally, the average light absorption contributions of BrC (± relative uncertainties) at 405 nm were quantified to be 11.7%(±5%), 6.3%(±4%), and 12.1%(±7%) in the campaigns of $urban_{\_winter}$, $urban_{\_fall}$, and $rural_{\_fall}$, respectively, and those at 532 nm were 10.0%(±2%), 4.1%(±3%), and 5.5%(±5%), respectively. The relatively higher BrC absorption contribution at 405 nm in the $rural_{\_fall}$ campaign could be reasonably attributed to the biomass burning events nearby, which was then directly supported by the biomass burning simulation experiments performed in this study. This paper indicates that the BrC contribution to total aerosol light absorption at shorter wavelengths is not negligible in the highly urbanized and industrialized PRD region.

Key words: Brown carbon (BrC), Black carbon (BC), Light absorption, Absorption Angstrom Exponent (AAE)

1. Introduction

Light absorbing carbonaceous aerosols including black carbon (BC) and brown

carbon (BrC) are the primary matters absorbing light in the atmosphere. The importance of BC has been widely recognized in recent decades due to its effects of radiative forcing on climate change, while the role of BrC is far from being well known (Jacobson, 2001; Hansen et al., 1997; Haywood et al., 1997; Ramanathan and Carmichael, 2008; Gadhavi and Jayaraman, 2010; Wang et al., 2014). BrC is organic carbon which can absorb light based on a variety of chemical structures like nitrated/polycyclic aromatics, phenols, humic-like substances and biopolymers, etc. (Jacobson MZ, 1999; Sun et al., 2011; Poschl, 2005). Main sources of BrC include biomass and biofuel burning, atmospheric humic-like substances (HULIS) from multiple phase actions, and photochemical oxidation of volatile organic compounds (VOCs) (Bond, 2001; Bergstrom et al., 2007; Alexander et al., 2015). South and East Asia are typical regions of atmospheric brown clouds (ABC) (Alexander et al., 2015). Biomass burning has been recognized as a significant contributor to ABC, including forest burning, crop waste burning, traditional religious activities and residential burning in those countries like India, China, Thailand, etc. (Venkataraman et al., 2006; Yan et al., 2006; Chakrabarty et al., 2013; Chakrabarty et al., 2014; Huang et al., 2012). BrC mainly absorbs light at UV and short-visible wavelengths (Chen and Bond, 2010; Kirchstetter et al., 2004; Lewis et al., 2008; Sandradewi et al., 2008; Schmid et al., 2006) and this strong spectral dependence has aroused more and more interest recently (Feng et al., 2013; Bahaduret al., 2012; Chung et al., 2012b; Wang et al., 2014; Jethva et al., 2011). BrC was ever estimated to contribute about 10–30% of total absorption of fine particles at shorter wavelengths, e.g., at 365 and 405 nm, and contribute approximately 10% at mid-visible wavelengths, e.g., at 532 nm (Bahadur et al., 2012; Lack et al., 2012b; Washenfelder et al., 2015; Nakayama et al., 2014). During an agricultural waste burning event, BrC aerosol could contribute more than 65% of light absorption at 370 nm and 15% at a mid-wavelength (Favez et al., 2009). However, the complexity and variety of molecular composition of BrC and the mixing state with other substances make it very challenging to study BrC optical properties (Alexander et al., 2015). Extensive experimental data from field studies are essential to evaluate light absorption by BrC as well as constraining and validating atmospheric and climate models.

There were two main methods to identify the absorption of BrC in total aerosol absorption at shorter wavelengths in previous studies: one was to use theoretical Mie models to calculate the light absorption of BrC with input of ambient chemical, physical, and optical measurements of bulk aerosol (Lack et al., 2012b); the other was based on optical measurement followed by absorption angstrom exponent (AAE) calculation, which was actually simpler and widely used with a criterion of AAE for "pure" BC aerosol ($AAE_{\_BC}$) (Clarke et al., 2007; Favez et al., 2009; Yang et al., 2009; Bahadur et al., 2012; Chung et al., 2012a). The $AAE_{\_BC}$ has been commonly assumed to be 1.0 theoretically in many studies, but this simple assumption may not be reliable, and could cause a possible bias of the attributed absorption of BC from –22% to +7% and then cause significant uncertainty of attributed BrC absorption (Lack and Langridge, 2013).

Some previous studies showed that ambient AAE was significantly affected by aerosol OC/EC (organic carbon/elemental carbon) ratio, suggesting a potentially important role of organic matter in aerosol light absorption (Utry et al., 2014). In this study, we tried to apply the AAE method to both urban and rural areas in the Pearl River Delta (PRD) region of China to attribute light absorption of BrC, with an emphasis of exploring realistic $AAE_{\_BC}$ based on on-line measurements in field campaigns. The PRD region is one of the three economically-developed regions of China and has been considered as one of the world's largest sources of anthropogenic soot emissions (Streets et al., 2001; Bond et al., 2004; Koch and Hasen, 2005). Despite of strong emissions of BC aerosol in the highly urbanized and industrialized PRD region, the light absorption contribution of BrC aerosol should not be neglected without effective evaluation. Therefore, the focus of this paper was to reasonably quantify the light absorption of BrC aerosol in PRD with effective uncertainty evaluation using the AAE method.

2. Experimental and data analysis methods

2.1 Sampling sites and periods

Our measurements contained three field campaigns conducted in Shenzhen and Heshan in PRD during fall and winter, which are usually the polluted dry seasons of PRD with high frequency of haze episodes. The Shenzhen site (SZ) was an urban site in the southeast of the PRD region. It was on the campus of Peking University Shenzhen Graduate School (22.60ºN, 113.97ºE), located in the west of Shenzhen, and the sampling periods were from 15th January to 19th February in the winter (urban$_{_winter}$) and from 12th September to 9th October in the fall (urban$_{_fall}$) in 2014. The Heshan site (HS) was a rural site (22.71°N, 112.93°E), 40–50 km southwest to the megacity of Guangzhou in the central PRD. It was located on the top of a small hill with little local fossil fuel combustion emission nearby except biomass burning. The HS sampling period was from 1st to 22th November in the fall (rural$_{_fall}$) in 2014 and biomass burning events were observed occasionally as an obvious anthropogenic source in the nearby farmland.

In addition, tunnel experiments were also performed in Shenzhen in 2014 to explore the AAE values in a highly BC-polluted environment. We performed tunnel experiments three times in Shenzhen urban areas: twice in the Tanglangshan tunnel (TL) and once in the Jiuweiling (JW) tunnel. The sampling periods of the Tanglangshan tunnel were from 0:00 am to 5:30 am on both 16th and 18th October (as the TL-1 and TL-2 experiments, respectively). The TL tunnel was 1.71 km in length with two channels that has three lanes in one direction for traffic, and the driving speeds in the tunnel were usually between 50–60 km/h. The monitoring car was located 400 m in depth from the entrance. The sampling period of the JW tunnel was from 3:30 pm to 24:00 pm on 10th December (as the JW experiment). The JW tunnel was 1.45 km in length with two channels that has two lanes in one direction for traffic, and the driving speeds in the tunnel were usually about 60 km/h. The monitoring car was located 800 m in depth from the entrance.

Moreover, since biomass burning is recognized as an important source of BrC (Ramanathan, et al., 2007) and is a popular source in rural areas in PRD, especially during the harvest season (He et al., 2011; Zhang et al., 2013), we performed biomass burning simulation experiments in a combustion laboratory to study the spectral dependence of aerosol light absorption in biomass burning smoke. Different types of biomass materials, including straw, deciduous leaf, and firewood, were burned in two different combustion modes, i.e., stove burning and open burning, to simulate the traditional residential and field biomass burning. The combustion system in the laboratory included four parts: combustion simulation, dilution, tube sampling, and instrumental analyzing. The stove was built with bricks and mortar according to the local traditional structure. More detailed information of the combustion system was described in our previous paper (He et al., 2010). Different biomass materials were burned inside the stove to simulate a complete water heating process referring to a standard protocol of water boiling test provided by the University of California (http://www.aprovecho.org/lab/pubs/testing). In addition, a certain amount of straw was piled up and burned on a pallet made of iron wire to simulate open burning of crop residues in the field.

2.2 Instrumentation

For the ambient sampling in this study, the instruments were placed in a temperature controlled room (or a monitoring car for the tunnel experiments), and the outdoor air was induced through a $PM_{2.5}$ cyclone inlet placed on the rooftop and then dried before it entered the inlets of the instruments. A three-wavelength Photo-acoustic Soot Spectrometer (PASS-3) (Droplet Measurement Technologies, CO, USA) was used to measure light absorption at 405, 532, and 781 nm with a data output time resolution of 2 min. The principles and technical details of PASS-3 were described previously by Arnott et al. (1999). Then, we processed the 2 min time resolution data of absorption at three wavelengths for half hour averages and made further data analysis based on the half hour time resolution datasets. On the other hand, we also processed the 10 min time resolution data of organic aerosol derived from AMS or ACSM for half hour

averages to explore the relationship with the absorption datasets.

A high-resolution time-of-flight aerosol mass spectrometer (HR-ToF-AMS) (Aerodyne Research, MA, US) was used to measure non-refractory species of PM_1 including organic aerosol with a time resolution of 10 min at the SZ site. The detailed description of the instrument was given by DeCarlo et al. (2006), and the calibration followed the standard protocols (Jayne et al., 2000; Jimenez et al., 2003; Drewnick et al., 2005). More details about the HR-ToF-AMS operation were described in our previous publications (He et al., 2011; Huang et al., 2011). An aerosol chemical speciation monitor (ACSM) (Aerodyne Research, MA, US) was used at the HS site and in the tunnel experiments with a time resolution of 10 min. In comparison with HR-ToF-AMS, ACSM was smaller and more convenient to be transported to field sampling sites and setup in a monitoring car with limited space. The detailed description of ACSM was given by Ng et al. (2011).

2.3 Calibration of PASS-3

The calibrations of PASS-3 for flow rate, laser power, and absorption were conducted following the standard procedures provided by the operational manual, which were also applied in relevant previous studies (Arnott et al., 2000; Lan et al., 2013; Nakayama et al., 2015). Firstly, the flow rate of sample air was calibrated by a soap film flow meter, with the results shown in Table 1; secondly, the laser power for each wavelength was calibrated by a laser power meter and the error in Table 1 indicated the reading difference between the laser power meter and the laser detector inside the instrument; thirdly, the light absorption calibration was performed by measuring highly absorbing NO_2 (200 ppm) at 532 nm. Then a good linear regression (with R^2>0.99) of the calculated extinction coefficient of NO_2 and the measured light absorption was established. Since the scattering of gas is negligible, the extinction of NO_2 should be very close to the absorption of NO_2, and thus the slope of the fitting curve should be very close to 1, as shown in Table 1. The detection limit of aerosol

light absorption with 2 s time resolution was 10, 10, and 3 Mm^{-1} at 405, 532, and 781 nm, respectively.

Table 1. The calibration results of PASS-3 in the campaigns.

Campaign	Flow rate (lpm)	Error of laser power_405 nm	Error of laser power_532 nm	Error of laser power_781 nm	Slope (R^2)
$Urban_{-winter}$	0.97	0.6 (%)	2.3 (%)	2.5 (%)	1.02 (0.995)
$Urban_{-fall}$	0.98	4.0 (%)	1.1 (%)	0.9 (%)	1.03 (0.996)
$Rural_{-fall}$	0.98	2.5 (%)	5.0 (%)	3.6 (%)	1.04 (0.993)
Tunnel	0.98	2.8 (%)	4.3 (%)	3.7 (%)	1.07 (0.993)

2.4 Calculation of AAE and light absorption of BrC

The AAE is an application of Angstrom exponent (Angstrom, 1929) to describe the wavelength dependence of visible light absorption by aerosol, as expressed in Equation 1:

$$AAE = -\ln(Abs_{\lambda 1}/Abs_{\lambda 2})/\ln(\lambda 1/\lambda 2) \quad (1)$$

Where Abs can be obtained by the absorption measurement and λ represents a wavelength. The traditional AAE method for estimating BrC light absorption was described previously by Lack and Langridge (2013), and it can be expressed in Equations 2 and 3:

$$BC\_Abs_{\lambda 1} = Abs_{\lambda 2} \times (\lambda 2/\lambda 1)^{AAE\_BC} \quad (2)$$

$$BrC\_Abs_{\lambda 1} = Abs_{\lambda 1} - BC\_Abs_{\lambda 1} \quad (3)$$

Where $Abs_{\lambda 2}$ is the measured absorption at a longer wavelength, at which BrC has negligible or no absorption. $BC\_Abs_{\lambda 1}$ is the attributed absorption of BC at a shorter wavelength. $BrC\_Abs_{\lambda 1}$ is thus the attributed absorption of BrC at the shorter wavelength. $AAE_{\_BC}$ is referred to as the AAE caused solely by "pure" BC aerosol, and is usually assumed to be 1.0 theoretically.

The total uncertainty of $BrC\_Abs_{\lambda 1}$ calculated (U_t) thus arises from both the absorption measurements and the AAE attribution method, and can be estimated by Equation 4:

$$U_t = \sqrt{\left(U_{Abs\_\lambda 1}\right)^2 + \left(U_{Abs\_\lambda 2}\right)^2 + \left(U_{AAE\_BC} \times \ln(\lambda 2/\lambda 1)\right)^2} \quad (4)$$

Where $U_{Abs\_\lambda 1}$ and $U_{Abs\_\lambda 2}$ are the relative uncertainties of the absorption measured at λ_1 and λ_2, respectively; U_{AAE_BC} is the absolute uncertainty of the $AAE_{\_BC}$ used, and needs to be multiplied by $\ln(\lambda_2/\lambda_1)$ to obtain the relative uncertainty of the AAE method. The uncertainty of the absorption measurement at a wavelength (U_{Abs_λ}) includes the fit to the absorption calibration slope, the electronic noise within the instrument (Lack et al., 2012a), as well as the drift correction of signals, and can be expressed as below:

$$\Delta X = \sqrt[2]{(\Delta X_{calibration})^2 + (\Delta X_{noise})^2 + (\Delta X_{drift})^2} \quad (5)$$

$$U_{Abs\_\lambda} = \Delta X / Abs_\lambda \quad (6)$$

Where $\Delta X_{calibration}$ is derived from the uncertainty of the regression slope under a 95% confidence level (p); ΔX_{noise} can be calculated through uncertainty propagation of noise equivalent absorption measured by PASS-3 every 2 minutes; ΔX_{drift} is the standard deviation of the averaged baseline absorption of filtered air. Finally, ΔX is divided by Abs_λ to get the corresponding relative uncertainty (U_{Abs_λ}). In result, the relative uncertainties of the absorption measurements at the three wavelengths were ~1.2% for the campaign of $urban_{\text{-winter}}$, 0.8–0.9% for the campaign of $urban_{\text{-fall}}$, and 1.5–1.6% for the campaign of $rural_{\text{-fall}}$.

3. Results and discussion

3.1 Aerosol light absorption

The time series of $PM_{2.5}$ light absorption at three wavelengths in different campaigns were shown in Fig.1. In the $urban_{\text{-winter}}$ campaign, the average absorption was 25.6, 18.7, and 12.9 Mm^{-1} at 405, 532, and 781 nm, respectively. In the $urban_{\text{-fall}}$ campaign, the average absorption was 21.6, 16.2, and 11.8 Mm^{-1} at 405, 532, and 781 nm, respectively. It was seen that the aerosol absorbed more light in the winter, and its

maximum absorptions were 162, 122, and 86.6 Mm^{-1} at 405, 532, and 781 nm, respectively, more than two times of the maximum values in the fall. The higher aerosol pollution observed in the winter could be attributed to the unfavorable meteorological conditions in PRD in the winter, when the air mass came from the polluted northern continent with a overwhelming frequency and the atmospheric boundary layer became shallower due to lower ambient temperatures (Huang et al., 2014). In the $rural_{\_fall}$ campaign, the average absorption was 32.5, 21.5, and 14.6 Mm^{-1} at 405, 532, and 781 nm, respectively, which were even higher than those of the $urban_{\_winter}$ and $urban_{\_fall}$ campaigns, but this was not strange since HS was a receptor site, suffering from the polluted air outflow from the northeast, where the megacity of Guangzhou was located, during the fall and winter seasons (Gong et al., 2012). The campaign-average ambient AAE_{405_781} values (± relative uncertainties) were calculated to be 1.05 (±0.01%), 0.92 (±0.10%), and 1.22 (±0.002%), respectively, for the $urban_{\_winter}$, $urban_{\_fall}$, and $rural_{\_fall}$ campaigns, while those of AAE_{532_781} were 0.98 (±0.01%), 0.82 (±0.05%), and 1.00 (±0.001%), respectively. The corresponding uncertainties in the brackets were calculated through the uncertainty propagation of the absorption measurement uncertainties based on Equation 1. The relatively higher values of AAE_{405_781} and AAE_{532_781} in the $rural_{\_fall}$ campaign might be related to the biomass burning in the farmland surrounding the HS site.

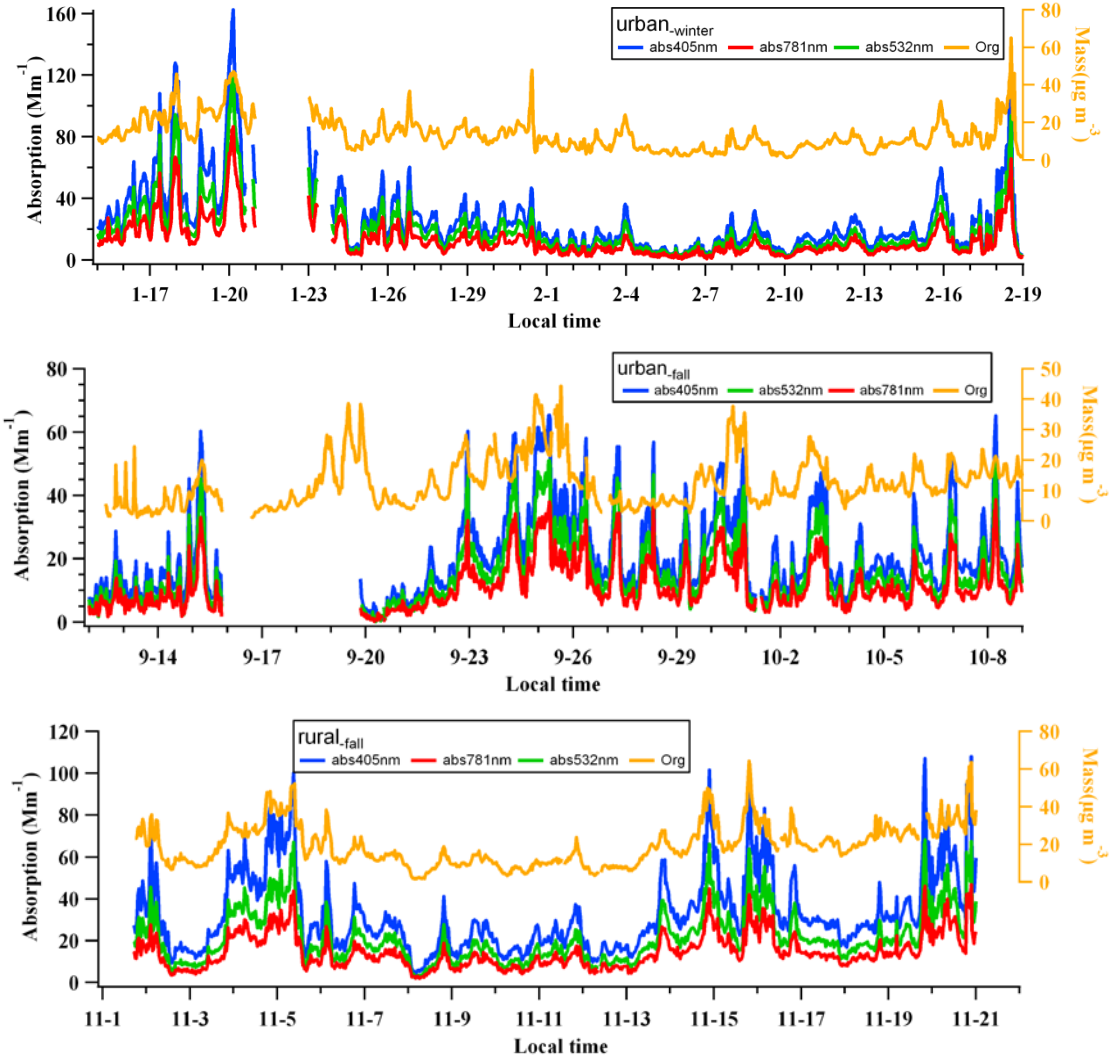

Fig.1. The time series of aerosol light absorption and mass concentration of organic aerosol in the different campaigns.

It should be noted here that the contribution of dust particles to the aerosol light absorption was considered to be negligible in this study. Firstly, there was no dust event during the three campaigns; secondly, organic aerosol typically contributes >30% of $PM_{2.5}$ mass in both urban and rural environments, far higher than that of the dust (<5%) (Huang et al., 2014). Considering that the mass absorption efficiency (MAE) values of dust at shorter and mid-visible wavelengths are lower than those of organic aerosol by a magnitude of one or two (Favez et al., 2009; Yang et al., 2009), the light absorption contribution of dust could be negligible in comparison with that of organic aerosol in PRD. Therefore, light absorption of dust was not taken into account in the

following discussion.

3.2 Determination of the AAE for "pure" BC aerosol

Theoretically, the AAE for "pure" BC aerosol ($AAE_{\_BC}$) is assumed to be 1.0 (Lack and Langridge, 2013), and BrC absorption at shorter wavelengths can raise this value in ambient atmosphere. In this study, we explored more realistic $AAE_{\_BC}$ in PRD by establishing a univariate regression relationship for each campaign, as shown in Fig. 2. In each campaign, the organic aerosol mass concentration was measured by AMS or ACSM, and the absorption at 781 nm (Abs_{781nm}) could be used to represent the BC amount since BrC had negligible absorption at longer wavelengths (Kirchstetter et al., 2004; Lack and Langridge, 2013; Lack et al., 2012b). Then, $r_{\_org/bc}$ (the ratio of organic aerosol mass concentration to Abs_{781nm}) was used as an index of the relative abundance of organic aerosol to BC. In our campaigns, $r_{\_org/bc}$ was a simpler while more effective index than other similar indices like the mass ratio of OC/(OC+EC), calculating which needed to assume a mass absorption efficiency for the measured light absorption data and correct the cutoff size difference for PASS-3 ($PM_{2.5}$) and AMS/ASCM (PM_1) sampling. Finally, the AAE_{405_781} and AAE_{532_781} were plotted versus the $r_{\_org/bc}$ averaged within equal intervals for each campaign in Fig. 2, with the corresponding linear fitting curves.

For all the campaigns, the linear relationships between AAE_{405_781} (or AAE_{532_781}) and $r_{\_org/bc}$ were significant enough with correlation coefficients (R^2) of 0.59–0.98, indicating AAE was positively related with the relative amount of organic matter, which certainly included BrC. Utry et al. (2014) also revealed a strong correlation between AAE and aerosol OC/EC at an urban site in Hungary, where OC was mainly emitted from wood burning and contained a large amount of BrC. The intercepts of the fitting curves in Fig.2, where $r_{\_org/bc}=0$, can be regarded as the situation for "pure" BC without any organic matter, and thus are suitable proxies of the $AAE_{\_BC}$ values for the different campaigns. The uncertainties of the regression intercepts represent the absolute uncertainties of the $AAE_{\_BC}$ (U_{AAE_BC}), and can be calculated following

Equation 7:

$$U_{AAE\_BC} = t_p \times S(a) \quad (7)$$

Where S(a) represents the standard deviation of the regression intercept (a) calculated by the SPSS software, and t_p is determined by the t-distribution list according to a confidence level (p), which was set to be 95% in this study.

The calculated $AAE_{\_BC}$ values and corresponding uncertainties at 405 and 532 nm were summarized in Table 2, and they were found similar in the $urban_{\text{-winter}}$ (0.86±0.06 and 0.70±0.05) and $urban_{\text{-fall}}$ (0.82±0.06 and 0.71±0.06) campaigns, but were higher in the $rural_{\text{-fall}}$ campaign (1.02±0.10 and 0.86±0.13). The difference of the $AAE_{\_BC}$ between the urban site and rural site might result from different sources of BC aerosol. Fossil fuel combustion, e.g., vehicle emissions, was indicated to be the dominant source of BC aerosol in urban Shenzhen (Lan et al., 2011), while biomass burning emissions played an important role in the fall at the rural HS site (Gong et al., 2012). In PRD, Lan (2013) ever found that the BC diameters of both vehicular exhaust and biomass burning were generally above 100 nm, using a single particle soot photometer to measure, and the BC diameters of vehicular emissions were even larger. On the other hand, Gyawali et al. (2009) found that the AAE value would decrease as the BC diameter increases in the range of 0.1–1 μm by theoretical modeling. Therefore, the larger $AAE_{\_BC}$ obtained at the rural site could be a result of the smaller BC diameters of biomass burning in PRD.

It should be noted that previous studies showed that AAE of ambient aerosol can also be influenced by a couple of other factors, such as size distribution, mixing state, and fractal dimension of BC particles (Levin et al., 2010; Gyawali et al., 2009; Scarnatol et al., 2013; Bond et al., 2006), but it is quite complicated and almost impossible to consider the influence of all these factors simultaneously. Scarnato et al. (2013) also pointed out that it is very difficult to clarify the relationship between AAE and aerosol morphology and mixing state due to quite complicated mechanisms in real cases. In

this study, this issue was just simplified using a univariate regression analysis to explore the relationship between ambient AAE and organic aerosol. In result, the good correlations obtained in Fig. 2 indicated that BrC itself could be the dominant factor leading to the variation of AAE, and thus the extrapolated intercept was a good surrogate for $AAE_{\_BC}$. The influence of other factors could be partly reflected by the error bars of the data points in Fig. 2 and the estimated uncertainty of the intercept (i.e., U_{AAE_BC}).

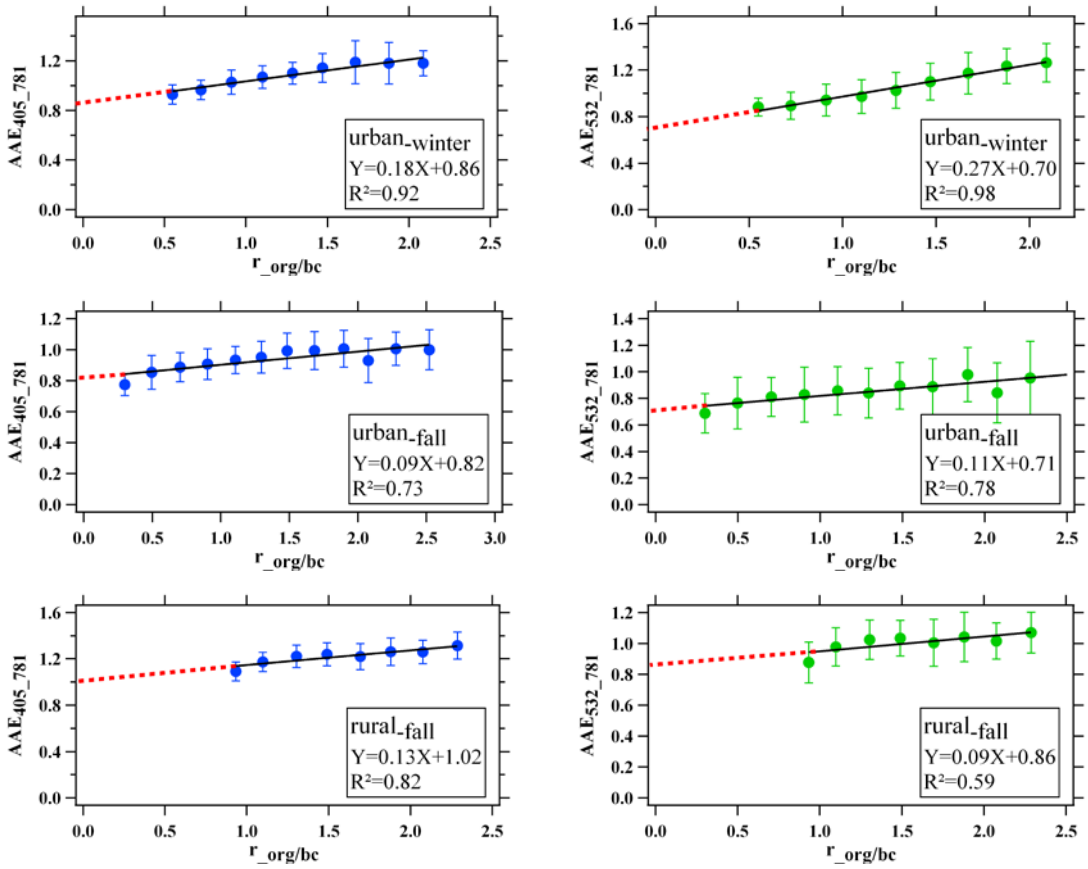

Fig.2. The linear relationship between AAE and $r_{\_org/bc}$ in the different campaigns.

Table 2. The derived $AAE_{\_BC}$ values and uncertainties in the different campaigns.

Campaign	AAE_{405_781}	AAE_{532_781}
$Urban_{\_winter}$	0.86±0.06	0.70±0.05
$Urban_{\_fall}$	0.82±0.06	0.71±0.06
$Rural_{\_fall}$	1.02±0.10	0.86±0.13

3.3 AAE measurements of primary emission sources

3.3.1 Roadway tunnel experiments

Since the major primary source of BC in urban environment in PRD was proved to be vehicular exhaust (Yuan et al., 2006; Huang et al., 2006; Lan et al., 2013), we performed three roadway tunnel experiments in urban Shenzhen, in order to verify the representativeness of the $AAE_{\_BC}$ derived from the urban atmosphere. The tunnel air measurement results were presented in Fig. 3. Since the tunnel air was largely dominated by fresh BC particles, the observed $r_{\_org/bc}$ values were found in a lower range (0.2–0.8) in comparison with those in the urban atmosphere, and thus the extrapolation of the linear regression in Fig. 3 could get more reliable intercepts, i.e., $AAE_{\_BC}$. As summarized in Table 3, the $AAE_{\_BC}$ values obtained at 405 and 532 nm (0.80–0.89 and 0.63–0.72, respectively) in the tunnel experiments well confirmed the $AAE_{\_BC}$ values derived from the ambient measurements in urban Shenzhen.

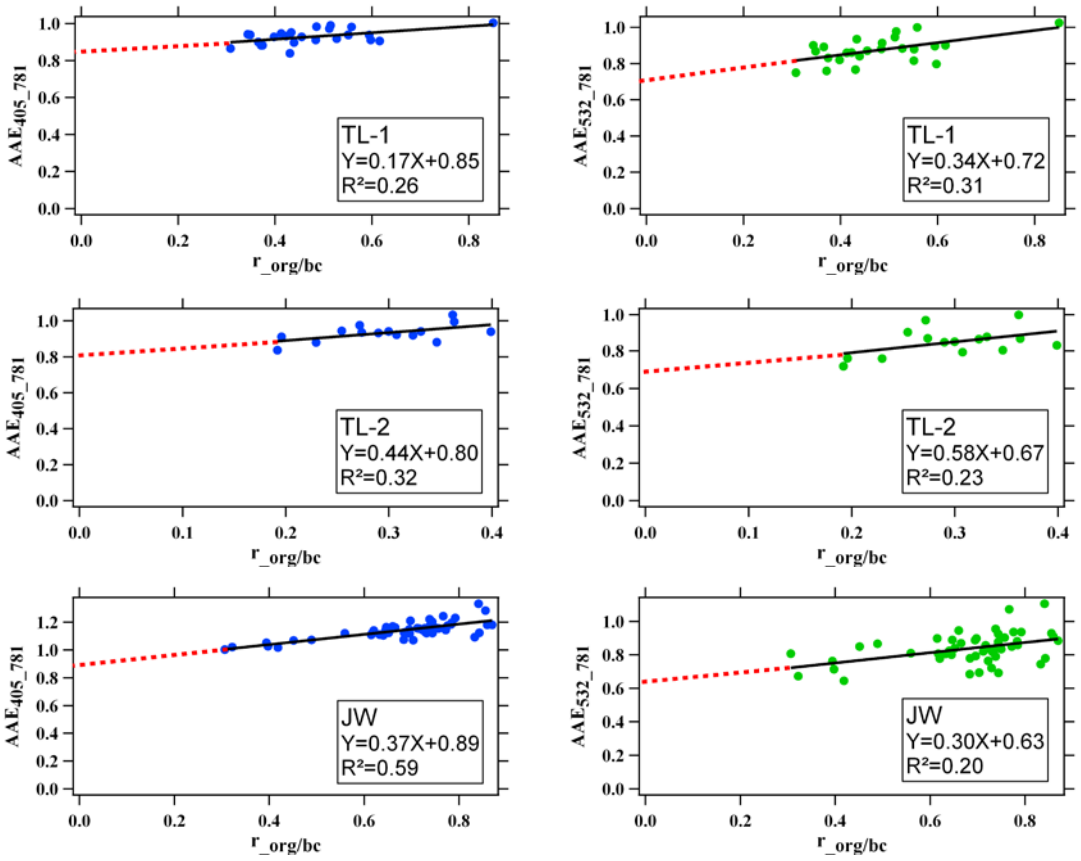

Fig.3. The linear relationship between AAE and $r_{\_org/bc}$ in the tunnel experiments.

Table 3. The derived $AAE_{\_BC}$ values and uncertainties in the tunnel experiments.

Tunnel	AAE_{405_781}	AAE_{532_781}
TL-1	0.85±0.06	0.72±0.10
TL-2	0.80±0.11	0.68±0.19
JW	0.89±0.06	0.63±0.12

370

371 3.3.2 Biomass burning simulation experiments

372 The AAE values with standard deviations of different types of biomass burning were
373 presented in Table 4. It was found that the absorption generally showed large spectral
374 dependence and the AAE varied among different biomass types or combustion modes,
375 with $AAE_{405\text{-}532}$ ranging from 2.1–8.3, $AAE_{532\text{-}781}$ ranging from 1.3–5.0, and
376 $AAE_{405\text{-}781}$ ranging from 1.7–6.2, significantly higher than those observed in the
377 ambient air and tunnel air. Therefore, the higher AAE values observed for biomass
378 burning particles, especially between 405 and 532 nm, proved that biomass burning
379 was a significant contributor to absorption at shorter wavelengths in the $rural_{\text{-}fall}$
380 campaign. In the combustion mode of stove burning, the leaves tended to emit more
381 BrC than wood, stalk, and straw, which should be a result of their different biomass
382 chemical nature. Besides, the AAE values of short straw were a few times higher in
383 open burning than in stove burning, which could be explained by that it was easier to
384 cause a hypoxic environment in smoldering and a larger amount of yellow fume was
385 produced (Einfeld et al., 1991; Patterson and McMahon, 1984; Kirchstetter et al.,
386 2004; Chakrabarty et al., 2010).

387

388 **Table 4.** The AAE values observed in the biomass burning simulation experiments.

Biomass type	Burning modes	AAE_{405_532}	AAE_{532_781}	AAE_{405_781}
Short straw	Open burning	8.27±1.34	4.96±1.15	6.20±1.33
Ficus microcarpa leaf	Stove burning	5.85±1.69	3.46±0.96	4.46±1.20
Lychee leaf	Stove burning	4.90±1.61	2.52±1.07	3.48±1.20
Corn stalk	Stove burning	3.83±1.49	2.39±1.06	2.97±1.16
Litchi wood	Stove burning	3.55±1.50	1.95±0.85	2.61±1.00
Eucalyptus wood	Stove burning	2.34±0.85	1.30±0.53	1.71±0.50
Short straw	Stove burning	2.32±0.65	1.39±0.47	1.76±0.25
Peanut stalk	Stove burning	2.13±1.01	2.08±0.86	1.99±0.50

389

390 3.4 Quantification of light absorption of BrC

Based on the well determined $AAE_{\_BC}$ and Abs_{781nm} in the three field campaigns, we could finally calculate the light absorption of BrC at 405 and 532 nm according to Equation 3. In result, the average light absorption of BrC at 405 nm was 3.0, 1.4, and 3.9 Mm^{-1} in the $urban_{\_winter}$, $urban_{\_fall}$, and $rural_{\_fall}$ campaigns, respectively, contributing 11.7%(±5%), 6.3%(±4%), and 12.1%(±7%) of the total aerosol light absorption, respectively. Here, the values in the brackets were the relative uncertainties calculated through Equation 4. The average light absorption of BrC at 532 nm was 1.9, 0.7, and 1.2 Mm^{-1} in the $urban_{\_winter}$, $urban_{\_fall}$, and $rural_{\_fall}$ campaigns, respectively, contributing 10.0%(±2%), 4.1%(±3%), and 5.5%(±5%) of the total aerosol light absorption, respectively.

The results indicated that no matter at the urban site or rural site in PRD, BC still played a dominant role in total aerosol light absorption at 405 and 532 nm, but the contribution of BrC was not negligible, with a fraction of up to 12%. The higher BrC contribution in the $urban_{\_winter}$ campaign than that in the $urban_{\_fall}$ campaign suggested that BrC could play a more important role in polluted continental air mass, since Shenzhen had a higher frequency of continental air mass from the north than that of marine air mass from the south in winter. On the other hand, the highest BrC contribution at 405 nm in the $rural_{\_fall}$ campaign could be attributed to the influence of biomass burning in the farmland nearby, which was supported by the biggest difference of BrC absorption between 405 and 532 nm: the AAE_{405_532} of BrC was calculated to be 1.7, 2.5, and 4.3 for the campaigns of $urban_{\_winter}$, $urban_{\_fall}$, and $rural_{\_fall}$, respectively. High AAE_{405_532} was found to be a feature in the biomass burning simulation experiments, as in Table 4. Especially strong absorption at 404 nm of biomass burning-emitted BrC was also found by Lack et al. (2012b). The lowest AAE_{405_532} of the $urban_{\_winter}$ campaign indicated that fossil fuel combustion, rather than biomass burning, seemed to be the major source of BrC in Shenzhen in winter.

Finally, it should be noted that it is unwise to calculate the light absorption

contribution of BrC at a specific time during the field campaigns, since the $AAE_{\_BC}$ derived for the whole case of a single campaign could have a large bias from the real $AAE_{\_BC}$ at that time, due to variations of the influencing factors, e.g., size distribution, mixing state, and morphology of BC particles.

4. Conclusions

In this study, an improved AAE method was used to estimate the light absorption of BrC at an urban site and a rural site in the PRD region of China in polluted seasons during 2014, based on ambient on-line measurements using PASS-3 and AMS (or ACSM). The obtained ambient AAE_{405_781} averages were 1.05, 0.92, and 1.22 in the three campaigns of $urban_{\text{-winter}}$, $urban_{\text{-fall}}$, and $rural_{\text{-fall}}$, respectively, while those for AAE_{532_781} were 0.98, 0.82, and 1.00, respectively. The linear regression between AAE_{405_781} (or AAE_{532_781}) and the ratio of organic aerosol to BC resulted in reasonable intercepts, which were assumed to be the AAE for "pure" BC ($AAE_{\_BC}$). The obtained $AAE_{\_BC}$ values between 405–781 nm were 0.86, 0.82, and 1.02 in the campaigns of $urban_{\text{-winter}}$, $urban_{\text{-fall}}$, and $rural_{\text{-fall}}$, respectively, and those between 532–781 nm were 0.70, 0.71, and 0.86, respectively. These $AAE_{\_BC}$ values were believed to be more realistic in PRD than the theoretical default value of 1.0. The results of the tunnel experiments further confirmed that the realistic $AAE_{\_BC}$ values in the urban atmosphere should be within the ranges of 0.8–0.9 between 405 and 781 nm and of 0.6–0.7 between 532 and 781 nm. In result, the average BrC light absorption contributions (± relative uncertainties) at 405 nm were quantified to be 11.7%(±5%), 6.3%(±4%), and 12.1%(±7%) in the campaigns of $urban_{\text{-winter}}$, $urban_{\text{-fall}}$, and $rural_{\text{-fall}}$, respectively, and those at 532 nm were 10.0%(±2%), 4.1%(±3%), and 5.5%(±5%), respectively. It was found that BrC played a more important role in more polluted winter or in the rural area with intensive biomass burning in PRD. Although BC still played a dominant role in total aerosol light absorption in PRD, the contribution of BrC at shorter wavelengths was not negligible, with a percent of up to >10%.

Acknowledgements

This work was supported by the National Natural Science Foundation of China (21277003 & U1301234), the Ministry of Science and Technology of China (2013CB228503), and the Science and Technology Plan of Shenzhen Municipality.

References

Alexander, L., Julia, L., Serger, A. N.: Chemistry of Atmospheric Brown Carbon, Chemical Reviews., Special Issue: Chemistry in Climate, 115, 4335-4382, DOI:10.1021/CR5006167,2015.

Ångström, A.: On the Atmospheric Transmission of Sun Radiation and on Dust in the Air, Geografika Ann., 11, 156–166, 1929.

Arnott, W. P., Moosmuller, H., Rogers, C. F., Jin, T. F., Bruch, R.: Photoacoustic spectrometer for measuring light absorption by aerosol: instrument description, Atmos. Environ., 33, 2845–2852, 1999.

Arnott, W. P., Moosmuller, H., Walker, J. W.: Nitrogen Dioxide and Kerosene-Flame Soot Calibration of Photoacoustic Instruments for Measurement of Light Absorption by Aerosols, Rev. Sci. Instrum., 71, 4545–4552, doi: 10.1063/1.1322585, 2000.

Arola, A., Schuster, G., Myhre, G., Kazadzis, S., Dey, S., Tripathi, N.: Inferring absorbing organic carbon content from AERONET data, Atmos. Chem. Phys., 11, 215–225, doi:10.5194/acp-11-215-2011, 2011.

Bahadur, E., Praveen, P. S., Xu, Y., Ramanathan, V.: Solar absorption by elemental and brown carbon determined from spectral observations, P. Natl. Acad. Sci., 109, 17366–17371, 2012.

Bergstrom, R. W., Pilewskie, P., Russell, P. B., Redemann, J., Bond, T. C., Quinn, P. K., Sierau, B.: Spectral absorption properties of atmospheric aerosols, Atmos. Chem. Phys., 7, 5937–5943, 2007.

Bond, T. C., Bergstrom, R.W.: Light Absorption by Carbonaceous Particles: An Investigative Review, Aerosol Sci. Technol., 40(1), 27–67, doi:10.1080/02786820500421521, 2006.

Bond, T. C., Streets, D. G., Yarber, K. F., Nelson, S. M., Woo, J. H., Klimont, Z.: A technology-based global inventory of black and organic carbon emissions from combustion, J. Geophys. Res., 109, D14203. doi:10.1029/2003jd003697, 2004.

Bond, T.C.: Spectral dependence of visible light absorption by carbonaceous particles emitted from coal combustion, Geophys. Res. Lett., 28, 4075–4078, 2001.

Chakrabarty, R. K., Arnold, I. J., Francisco, D. M., Hatchett, B., Hosseinpour, F., Loria, M., Pokharel, A., Woody, B. M.: Black and brown carbon fractal aggregates from combustion of two fuels widely used in Asian rituals, Journal of Quantitative Spectroscopy & Radiative Transfer., 122, 25–30, doi:10.1016/j.jqsrt.2012.12.011, 2013.

Chakrabarty, R. K., Moosmuller, H., Chen, L. W. A., Lewis, K., Arnott, W. P., Mazzoleni, C., Dubey, M. K., Wold, C. E., Hao, W. M., Kreidenweis, S. M.: Brown carbon in tar balls from smoldering biomass combustion,

Atmos. Chem. Phys., 10, 6363–6370, doi:10.5194/acp-10-6363-2010, 2010.

Chakrabarty, R. K., Pervez, S., Chow, J. C., Watson, J. G., Dewangan, S., Robles, J., Tian, G. X.: Funeral Pyres in South Asia: Brown Carbon Aerosol Emissions and Climate Impacts, Environ. Sci. Technol. Lett., 1, 44-48, doi: 10.1021/ez4000669, 2014.

Chen, Y., Bond, T. C.: Light absorption by organic carbon from wood combustion, Atmos. Chem. Phys., 10, 1773-1787, 2010.

Chung, C. E., Kim, S. W., Lee, M., Yoon, S. C., Lee, S.: Carbonaceous aerosol AAE inferred from in-situ aerosol measurements at the Gosan ABC super site, and the implications for brown carbon aerosol, Atmos. Chem. Phys., 12, 6173–6184, doi:10.5194/acp-12-6173-2012, 2012a.

Chung, C. E., Ramanathan, V., Decremer, D.: Observationally constrained estimates of carbonaceous aerosol radiative forcing, P. Natl. Acad. Sci., 109(29), 11624-11629, 2012b.

Clarke, A., McNaughton, C., Kapustin, V., Shinozuka, Y., Howell, S., Dibb, J., Zhou, J., Anderson, B., Brekhovskikh, V., Turner, H., and Pinkerton, M.: Biomass Burning and Pollution Aerosol over North America: Organic Components and Their Influence on Spectral Optical Properties and Humidification Response, J. Geophys. Res., 112, D12S18, doi: 10.1029/2006jd007777, 2007.

DeCarlo, P. F., Kimmel, J. R., Trimborn, A., Northway, M. J., Jayne, J. T., Aiken, A. C., Gonin, M., Fuhrer, K., Horvath, T., Docherty, K. S., Worsnop, D. R., Jimenez, J. L.: Field-Deployable, High-Resolution Time-of-Flight Aerosol Mass Spectrometer, Anal. Chem., 78, 8281–8289, 2006.

Drewnick, F., Hings, S. S., DeCarlo, P., Jayne, J. T., Gonin, M., Fuhrer, K., Weimer, S., Jimenez, J. L., Demerjian, K. L., Borrmann, S., Worsnop, D. R.: A new time-of-flight aerosol mass spectrometer (TOF-AMS)–Instrument description and first field deployment, Aerosol. Sci. Tech., 39, 637–658, 2005.

Einfeld, W., Ward, D. E., and Hardy, C.: Effects of fire behavior on prescribed fire smoke characteristics: A case study, in: Global biomass burning: Atmospheric, climatic, and biospheric implications, MIT Press, Cambridge, MA, USA, 412–419, 1991.

Favez, O., Alfaro, S. C., Sciare, J., Cachier, H., Abdelwahab, M. M.: Ambient measurements of light-absorption by agricultural waste burning organic aerosols, J. Aerosol. Sci ., 40, 613–620, 2009.

Feng, Y., Ramanathan, V., Kotamarthi, V. R.: Brown carbon: a significant atmospheric absorber of solar radiation? Atmos. Chem. Phys., 13(17), 8607-8621, 2013.

Gadhavi, H., Jayaraman, A.: Absorbing aerosols: contribution of biomass burning and implications for radiative forcing, Ann. Geophys., 28, 103–111, doi:10.5194/angeo-28-103-2010, 2010.

Gong, Z. H., Lan, Z. J., Xue, L., Zeng, L. W., He, L. Y., Huang, X. F.: Characterization of submicron aerosols in the urban outflow of the central Pearl River Delta region of China, Environ. Sci. Eng., 6(5): 725–733, 2012.

Gyawali, M., Arnott, W. P., Lewis, K., Moosmüller, H.: In situ aerosol optics in Reno, NV, USA during and after the summer 2008 California wildfires and the influence of absorbing and non-absorbing organic coatings on spectral light absorption, Atmos. Chem. Phys., 9, 8007–8015, doi:10.5194/acp-9-8007-2009, 2009.

Hansen, J., Sato, M., Ruedy, R.: Radiative forcing and climate response, J. Geophys. Res., 102, 6831-6864, 1997.

Haywood, J. M., Roberts, D. L., Slingo, A., Edwards, J. M., Shine, K. P.: General circulation model calculations of

the direct radiative forcing by anthropogenic sulfate and fossil-fuel soot aerosol, Journal of Climate., 10, 1562-1577, 1997.

He, L. Y., Huang, X. F., Xue, L., Hu, M., Lin, Y., Zheng, J., Zhang, R. Y., Zhang, Y. H.: Submicron aerosol analysis and organic source apportionment in an urban atmosphere in Pearl River Delta of China using high-resolution aerosol mass spectrometry, J. Geophys. Res., 116 (D12304), DOI: 10.1029/2010JD014566, 2011.

He, L. Y., Lin, Y., Huang, X. F., Guo, S., Xue, L., Sun, Q., Hu, M., Luan, S. J., Zhang, Y. H.: Characterization of high-resolution aerosol mass spectra of primary organic aerosol emissions from Chinese cooking and biomass burning, Atmos. Chem. Phys., 10, 11535–11543, 2010.

He, M., Zheng, J. Y., Yin, S. S., Zhang, Y. Y.: Trends, temporal and spatial characteristics, and uncertainties in biomass burning emissions in the Pearl River Delta, China, Atmos. Environ.,45, 4051-4059, doi:10.1016/j.atmosenv.2011.04.016, 2011.

Huang, X. F., He, L. Y., Hu, M., Canagaratna, M. R., Kroll, J. H., Ng, N. L., Zhang, Y. H., Lin, Y., Xue, L., Sun, T. L., Liu, X. G., Shao, M., Jayne, J. T., Worsnop, D. R.: Characterization of submicron aerosols at a rural site in Pearl River Delta of China using an aerodyne high-resolution aerosol mass spectrometer, Atmos. Chem. Phys., 11(5): 1865–1877, 2011.

Huang, X. F., Sun, T. L., Zeng, L. W., Yu, G. H., Luan, S. J.: Black carbon aerosol characterization in a coastal city in South China using a single particle soot photometer, Atmos. Environ.,51, 21-28, 2012.

Huang, X. F., Yun, H., Gong, Z. H., Li, X., He, L. Y., Zhang, Y. H., Hu, M.: Source apportionment and secondary organic aerosol estimation of PM2.5 in an urban atmosphere in China, Science China: Earth Sciences., 57, 1352–1362, 2014.

Jacobson, M. Z.: Isolating nitrated and aromatic aerosols and nitrated aromatic gases as sources of ultraviolet light absorption. J. Geophys. Res., 104:3527–3542, 1999.

Jacobson, M. Z.: Strong radiative heating due to the mixing state of black carbon in atmospheric aerosols, Nature 409, 695-697, 2001.

Jayne, J. T., Leard, D. C., Zhang, X. F., Davidovits, P., Smith, K. A., Kolb, C. E., Worsnop, D. R.: Development of an aerosol mass spectrometer for size and composition analysis of submicron particles, Aerosol. Sci. Tech., 33, 49–70, 2000.

Jethva, H., Torres, O.: Satellite-based evidence of wavelength-dependent aerosol absorption in biomass burning smoke inferred from Ozone Monitoring Instrument, Atmos. Chem. Phys., 11, 10541–10551, doi:10.5194/acp-11-10541-2011, 2011.

Jimenez, J. L., Jayne, J. T., Shi, Q., Kolb, C. E., Worsnop, D. R., Yourshaw, I., Seinfeld, J. H., Flagan, R. C., Zhang, X. F., Smith, K. A., Morris, J. W., Davidovits, P.: Ambient aerosol sampling using the Aerodyne Aerosol Mass Spectrometer, J. Geophys. Res., 108, 8425, D7, doi:10.1029/2001JD001213, 2003.

Kirchstetter, T. W., Novakov, T., Hobbs, P. V.: Evidence that the spectral dependence of light absorption by aerosols is affected by organic carbon. J. Geophys. Res., 109, D21, doi:10.1029/2004JD004999, 2004.

Koch, D., Hansen, J.: Distant origins of Arctic black carbon: a Goddard Institute for Space Studies ModelE experiment, J. Geophys. Res., 110, D04204, doi:10.1029/2004jd005296, 2005.

Lack, D. A., Cappa, C. D., Cross, E. S., Massoli, P., Ahern, A. T., Davidovits, P., Onasch, T. B. : Absorption Enhancement of Coated Absorbing Aerosols: Validation of the Photo-Acoustic Technique for Measuring the Enhancement, Aerosol Sci. Tech., 43, 1006–1012, 2009.

Lack, D. A., Langridge, J. M., Bahreini, R., Cappa, C. D., Middlebrook, A. M., and Schwarz, J. P.: Brown carbon and internal mixing in biomass burning particles, P. Natl. Acad. Sci. USA. 109, 37, 14802-14807, doi:10.1073/pnas.1206575109, 2012b.

Lack, D. A., Langridge, J. M.: On the attribution of black and brown carbon light absorption using the Ångström exponent, Atmos. Chem. Phys., 13, 5089–5101, 2013.

Lack, D. A., Langridge, J., Richardson, M., Cappa, C. D., Law, D., Murphy, D. M.: Aircraft instrumentation for comprehensive characterization of aerosol optical properties, Part 2: Black and brown carbon absorption and absorption enhancement measured with photo acoustic spectroscopy, Aerosol Sci. Tech., 46, 555–568, 2012a.

Lack, D. A., Moosmüller, H., McMeeking, G. R., Chakrabarty, R. K., Baumgardner, D.: Characterizing elemental, equivalent black, and refractory black carbon aerosol particles: a review of techniques, their limitations and uncertainties, Anal Bioanal Chem., 406:99–122, doi:10.1007/s00216-013-7402-3, 2014.

Lan, Z. J., Chen, D. L., Li, X., Huang, X. F., He, L. Y., Deng, Y. G., Feng, N., Hu, M.: Modal characteristics of carbonaceous aerosol size distribution in an urban atmosphere of South China, Atmospheric Research., 100, 51-60, 2011.

Lan, Z. J., Huang, X. F., Yu, K. Y., Sun, T. L., Zeng, L. W., Hu, M.: Light absorption of black carbon aerosol and its enhancement by mixing state in an urban atmosphere in South China, Atmos. Environ., 69,118-123, 2013.

Lan, Z. J.: Characteristics of mixing state and light absorption of black carbon aerosol in China, PhD dissertation, Peking University., 2013.

Levin, E. J. T., McMeeking, G. R., Carrico, C. M., Mack, L. E., Kreidenweis, S. M. Word, C. E., Moosmuller, H., Arnott, W. P., Hao, W. M., Cottett Jr, J. L., Malm, W. C.: Biomass burning smoke aerosol properties measured during Fire Laboratory at Missoula Experiments (FLAME), J. Geophys. Res., Atmos 115:D182010, DOI: 10.1029/2009JD013601, 2010.

Lewis, K., Arnott, W. P., Moosmuller, H., Wold, C. E.: Strong spectral variation of biomass smoke light absorption and single scattering albedo observed with a novel dual-wavelength photoacoustic instrument, J. Geophys. Res., 113, D16, DOI: 10.1029/2007JD009699, 2008.

Moosmuller, H., Arnott, W. P., Rogers, C. F., Chow, J. C., Frazier, C. A., Sherman, L. E., Dietrich, D. L.: Photoacoustic and filter measurements related to aerosol light absorption during the Northern Front Range Air Quality Study (Colorado 1996/1997), J. Geophys. Res., 103(D21), 28149-28157, 1998.

Nakayama, T., Ikeda, Y., Sawada, Y., Setoguchi, Y., Ogawa, S., Kawana, K., Mochida, M., Ikemori, F., Matsumoto, K., Matsumi, Y.: Properties of light-absorbing aerosols in the Nagoya urban area, Japan, in August 2011 and January 2012: Contributions of brown carbon and lensing effect, J. Geophys. Res. Atmos., 119, 12,721–12,739, doi:10.1002/ 2014JD021744, 2014.

Nakayama, T., Suzuki, H., Kagamitani, S., Ikeda, Y.: Characterization of a three wavelength photoacoustic soot spectrometer (PASS-3) and photoacoustic extinctiometer (PAX), J. Meteorol. Soc. Jpn., 93, 285–308, doi: 10.2151/jmsj.2015-016, 2015.

Ng, N. L., Herndon, S. C., Trimborn, A., Canagaratna, M. R., Croteau, P. L., Onasch, T. B., Sueper, D., Worsnop, D. R., Zhang, Q., Sun, Y. L., Jayne, J. T.: An Aerosol Chemical Speciation Monitor (ACSM) for routine monitoring of the composition concentrations of ambient aerosol, Aerosol Sci. Tech., 45, 770-784, 2011..

Patterson, E. M., McMahon, C. K.: Absorption characteristics of forest fire particulate matter, Atmos. Environ., 18, 2541– 2551, 1984.

Poschl, U.: Atmospheric Aerosols: Composition, Transformation, Climate, and Health Effects, Atoms. Chem., 44, 7520-7540, 2005.

Ramanathan, V., Carmichael, G.: Global and regional climate changes due to black carbon, Nature Geoscience., 1, 221-227, 2008.

Ramanathan, V., Ramana, M.V., Roberts, G., Kim, D., Corriganm, C., Chung, C., Winker, D.: Warming trends in Asia amplified by brown cloud solar absorption. Nature 448, 575-578, doi:10.1038/nature06019 , 2007.

Sandradewi, J., Prevot, A. S. H., Weingartner, E., Schmidhauser, R., Gysel, M., Baltensperger, U.: A study of wood burning and traffic aerosols in an Alpine valley using a multi-wavelength Aethalometer, Atmos. Environ.,42, 101-111, 2008.

Scarnato, B. V., Vahidinial, S., Richard, D. T., Kirchstetter, T. W.: Effects of internal mixing and aggregate morphology on optical properties of black carbon using a discrete dipole approximation model, Atmos. Chem. Phys., 13, 5089–5101, 2013.

Schmid, O., Artaxo, P., Arnott, W. P., Chand, D., Gatti, L. V., Frank, G. P., Hoffer, A., Schnaiter, M., Andreae, M. O.: Spectral light absorption by ambient aerosols influenced by biomass burning in the Amazon Basin. I: comparison and field calibration of absorption measurement techniques. Atmos. Chem. Phys., 6, 3443-3462, 2006.

Streets, D. G., Gupta, S., Waldhoff, S. T., Wang, M. Q., Bond, T. C., Bo, Y. Y.: Black carbon emissions in China, Atmos. Environ., 35, 4281-4296, 2001.

Sun, H., Biedermann, L., Bond, T. C.: Color of brown carbon: A model for ultraviolet and visible light absorption by organic carbon aerosol, Geophys. Res. Lett., 34:L17813, DOI:10.1029/2007GL029797, 2007.

Utry, N., Ajtai, T., Pinter, M., Torok, Z., Bozoki, Z., Szabo, G.: Correlations between absorption Angström exponent (AAE) of wintertime ambient urban aerosol and its physical and chemical properties, Atmos. Environ., 91, 52-59, doi: 10.1016/j.atmosenv.2014.03.047, 2014

Venkataraman, C., Habib, G., Kadamba, D., Shrivastava, M., Leon, J.-F., Crouzille, B., Boucher, O., Streets, D. G.: Emissions from open biomass burning in India: Integrating the inventory approach with high-resolution Moderate Resolution Imaging Spectroradiometer (MODIS) active-fire and land cover data, Global Biogeochemical Cycles., 20, GB2013, doi:10.1029/2005GB002547, 2006.

Wang, X., Heald, C. L., Ridley, D. A., Schwarz, J. P., Spackman, J. R., Perring, A. E., Clarke, A. D.: Exploiting simultaneous observational constraints on mass and absorption to estimate the global direct radiative forcing of black carbon and brown carbon, Atmos. Chem. Phys., 14(20), 10989-11010, 2014.

Washenfelder, R. A., Attword, A. R., Brock, C. A., Guo, H., Xu, L., Weber, R. J., Ng, N. L., Allen, H. M., Ayres, B. R., Baumann, K., Cohen, R. C., Draper, D. C., Duffey, K. C., Edgerton, E., Fry, J. L., Hu, W. W., Jimenez, J. L., Palm, B. B., Romer, P., Stone, E. A., Wooldridge, P. J., Brown, S. S.: Biomass burning dominates brown

carbon absorption in the rural southeastern United States, Geophys. Res. Lett., 42, 653-664, DOI: 10.1002/2014GL062444, 2015.

Yan, X. Y., Ohara, T., Akimoto, H.: Bottom-up estimate of biomass burning in mainland China, Atmos. Environ., 40, 5262-5273, doi:10.1016/j.atmosenv.2006.04.040, 2006.

Yang, M., Howell, S. G., Zhuang, J., Huebert, B. J.: Attribution of aerosol light absorption to black carbon, brown carbon, and dust in China – interpretations of atmospheric measurements during EAST-AIRE, Atmos. Chem. Phys., 9, 2035–2050, doi:10.5194/acp-9-2035-2009, 2009.

Yuan, Z. B., Lau, A. K. H., Zhang, Y. H., Yu, J. Z., Louie, P. K. K., Fung, J. C. H.: Identification and spatiotemporal variations of dominant PM10 sources over Hong Kong, Atmos. Environ., 40: 1803–1815, 2006.

Zhang, Y. H., Hu, M., Liu, S. C., Wiedensohler, A.: The special issue on PRIDE-PRD2004 campaign, Atmos. Environ., 42 (25): 6155–6156, 2008.

Zhang, Y. S., Shao, M., Lin, Y., Luan, S. J., Mao, N., Chen, W. T., Wang, M.: Emission inventory of carbonaceous pollutants from biomass burning in the Pearl River Delta Region, China, Atmos. Environ., 76, 189-199, doi: 10.1016/j.atmosenv.2012.05.055, 2013.